Molecular Crystals and Liquid Crystals
Publication details, including instructions for authors and subscription information:
http://www.tandfonline.com/loi/gmcl20

Density Functional Theory (DFT) Study on the Addition of Hydroxyl Radical (OH) to C_{20}

Tetsuji Iyama [a], Shigeaki Abe [b] & Hiroto Tachikawa [a]

[a] Division of Materials Chemistry, Graduate School of Engineering, Hokkaido University, Sapporo, 060-8628, Japan

[b] Department of Biomedical, Dental Medicals and Engineering, Graduate School of Dental Medicine, Hokkaido University, Sapporo, 060-8586, Japan

Version of record first published: 17 Sep 2012.

To cite this article: Tetsuji Iyama , Shigeaki Abe & Hiroto Tachikawa (2012): Density Functional Theory (DFT) Study on the Addition of Hydroxyl Radical (OH) to C_{20} , Molecular Crystals and Liquid Crystals, 567:1, 200-206

To link to this article: http://dx.doi.org/10.1080/15421406.2012.703808

Mol. Cryst. Liq. Cryst., Vol. 567: pp. 200–206, 2012

ISSN: 1542-1406 print/1563-5287 online
DOI: 10.1080/15421406.2012.703808

Taylor & Francis
Taylor & Francis Group

Density Functional Theory (DFT) Study on the Addition of Hydroxyl Radical (OH) to C_{20}

TETSUJI IYAMA,[1] SHIGEAKI ABE,[2] AND HIROTO TACHIKAWA[1,*]

[1]Division of Materials Chemistry, Graduate School of Engineering, Hokkaido University, Sapporo 060-8628, Japan
[2]Department of Biomedical, Dental Medicals and Engineering, Graduate School of Dental Medicine, Hokkaido University, Sapporo 060-8586, Japan

The radical addition to the smallest fullerene C_{20} has been investigated by means of density functional theory (DFT) method in order to elucidate the radical scavenge mechanism of fullerene. The OH radical was examined as an organic radical because the radical has a high reactivity. The DFT calculation showed that the OH radical binds directly to the carbon atom of C_{20} and a strong C-O bond is formed. The binding energies of the first addition of OH radical were calculated to be 85.2 kcal/mol at the B3LYP/6-311G(d,p) level of theory. In the second radical addition, the binding energy of OH to C_{20}(OH) was 91.5 kcal/mol. The unpaired electron was distributed widely over the C_{20} surface in the C_{20}(OH) complex.

Keywords fullerene; DFT; radical addition; OH; hyperfine

1. Introduction

Fullerene and related compounds have some potential biological effects, e.g. antiviral activity, specific cleavage of DNA, inhibition of HIV protease, and photodynamic therapy [1], which has attracted considerable attention and has become a challenging research field. However, the fullerene is not soluble in water. The fullerol of C_{60}, hydroxyl radical isFigure 1 added to C_{60}, is one of the water-soluble fullerene derivatives to be suitable for biological study.

Electron spin resonance (ESR) spectroscopy and spin-trapping technique have proved that fullerol of C_{60} can efficient scavenge active oxygen radicals such as superoxide radical (O_2^-) [2] and hydroxyl radical (OH) [3]. Using time-resolved technique of laser photolysis, Lu et al. found that fullerol of C_{60} exists in aqueous solution and fullerol of C_{60} reacts with the primary irradiated products of water radiolysis [4]. Zeynalov Table 1investigated to determine the rate constants for addition of radicals to fullerenes [5].

C_{20} is the smallest fullerene which behaves a radical scavenger [6]. The reactions of C_{20} with radical species are a prototype of radical scavenger reaction. Therefore, the elucidation of reaction mechanism of C_{20} may shed light on the complicated reaction of C_{60}.

*Address correspondence to Hiroto Tachikawa Division of Materials Chemistry, Graduate School of Engineering, Hokkaido University Sapporo Tel.: 060-8628, Japan Fax: +81-11-706-7897. E.mail: hiroto@eng.hokudai.ac.jp

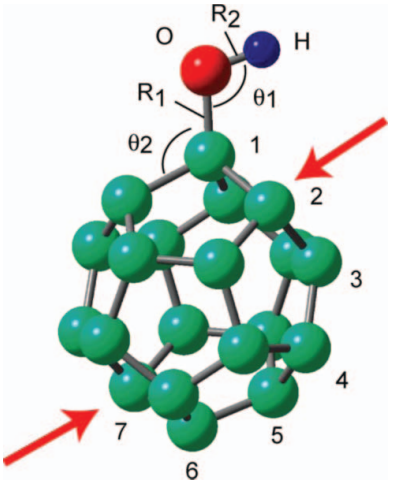

Figure 1. Optimized structure of C_{20}(OH) calculated at the B3LYP/6-311G(d,p) level. Numbers indicate carbon atom on C_{20}. Arrow means active sites of C_{20} in the second OH addition (2 and 7 carbon atoms).

In the present study, density functional theory (DFT) method is applied to the interaction system of C_{20} with hydroxyl radical (OH). The reaction of radical addition to C_{20} is investigated using potential energy calculation.

2. Method of Calculations

The C_{20} fullerene molecule and hydroxyl radical (OH) were examined as a fullerene and radical, respectively. The structures of C_{20} and OH radical adduct, C_{20}(OH), were fully optimized at the B3LYP/6–31G(d) and B3LYP/6-311G(d,p) levels of theory. The atomic charges were calculated using the natural bond population analysis (NPA) method at the B3LYP/6-31G(d) level.

All density functional theory (DFT) calculations were carried out using Gaussian 03 program package [7]. Previous studies showed that this level of theory give a reasonable electronic structure of carbon systems [8-17]. Electron spin operator $<S^2>$ values of C_{20}(OH) were less than 0.765 at all points. The basis set super position error (BSSE) was estimated by the counter poise method at the B3LYP/6-311G(d,p) level.

Table 1. Optimized parameters of C_{20}(OH).

Parameter	B3LYP/6-311G(d,p)
R_1	1.390
R_2	0.96
θ_1	108.1
θ_2	120.5

3. Results

3.1. Structure and electronic states of C_{20}(OH)

The optimized structure of C_{20}(OH) is illustrated in and optimized parameters are given in . The C-OH and O-H distances are calculated to be $R_1 = 1.392$ and $R_2 = 0.964$ Å at the B3LYP/6-311G(d,p) level, respectively. The O-H distance of the free OH radical is 0.975 Å, indicating that the O-H bond is shortened by the addition to the surface of C_{20}. The binding energies of OH radical to C_{20} was calculated to be 85.2 kcal/mol at the B3LYP/6-311G(d,p) level and 87.0 kcal/mol at the B3LYP/6-31G(d) level. After the basis set super position error (BSSE) correction, the binding energy was changed to 80.8 kcal/mol.

3.2. Interaction of C_{20} with the OH radical

Potential energy curves are plotted in Figure 2 as a function of R(C-OH). Zero level of energy corresponding to total energy of C_{20}(OH) at the optimized geometry. At intermolecular separation of R(C-OH) = 4.0 Å (**point a**), the energy is +97.0 kcal/mol relative to the zero level. The shape of potential energy curves show that the interaction of OH radical with C_{20} is composed of two electronic states. At the entrance region (**points a and b**), potential energy is flat and slightly repulsive. At inner region (**points c**), the potential energy curve shows attractive and the energy is minimized at R(C-OH) = 1.395 Å. This is due to the electronic state of OH radical is changed from π- to σ-types at the crossing region.

The spacial distributions of spin density on C_{20}-OH system at selected points are illustrated in Figure 3. At **points a and b**, the unpaired electron is mainly distributed on the

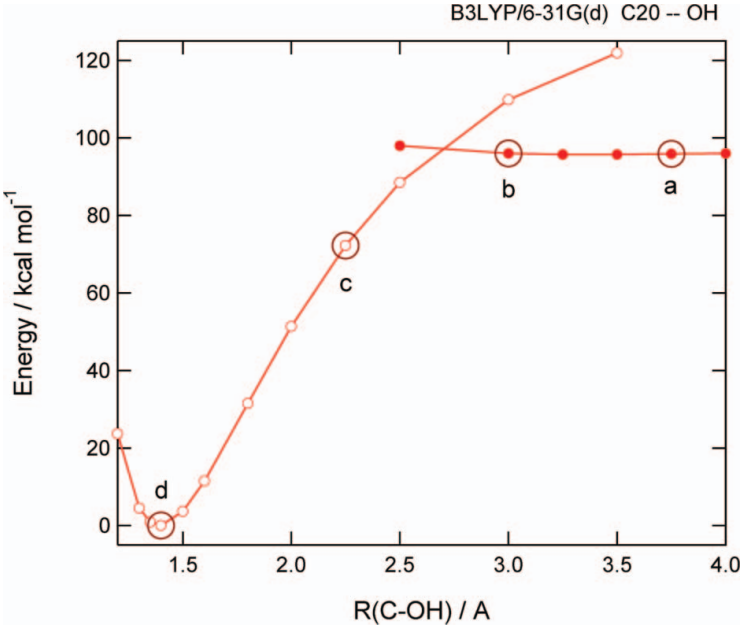

Figure 2. Potential energy curves for OH radical approaching to C_{20} surface. Values were calculated at the B3LYP/6-31G(d) level.

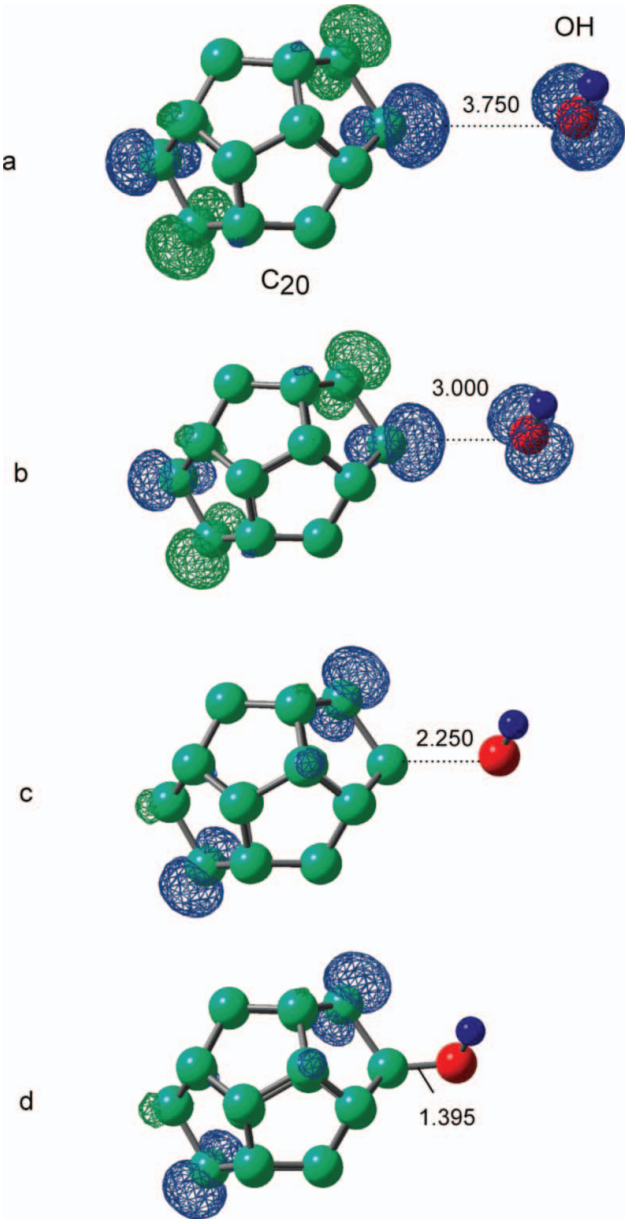

Figure 3. Spacial distribution of spin densities on C_{20}(OH). The positions of OH radical are R_1 = (C-OH) = 3.75 Å (a) 3.00 Å (b), 2.25 Å (c) and 1.395 Å (d). Calculation was carried out at the UB3LYP/6-31G (d) level.

OH radical, although the spin is slightly contaminated into the C_{20} surface. On the other hand, the spin density is only distributed on C_{20} near optimized structure.

The hyperfine coupling constant of proton (H-hfcc) gives an important information on the electronic states of radicals. The H-hfcc's of C_{20}(OH) and free OH radical were calculated to be −0.11 and −23.89 G, respectively. This result indicates that theFigure 4

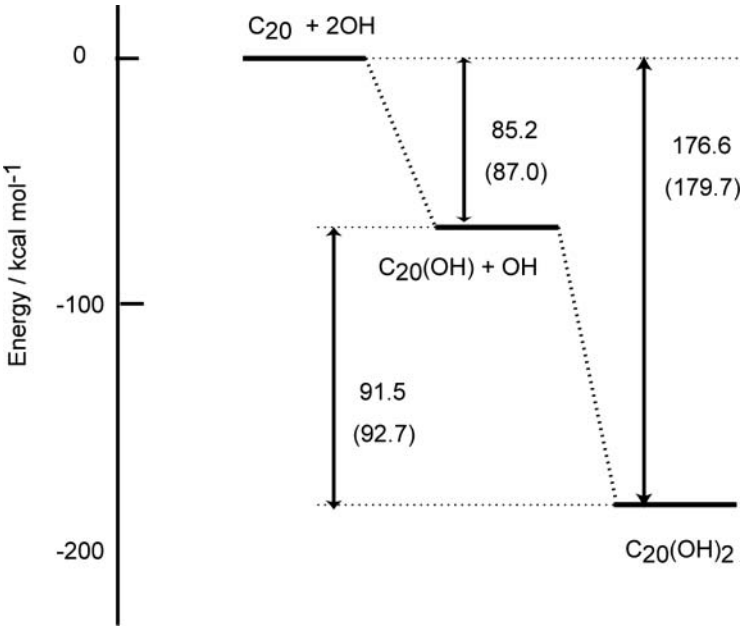

Figure 4. Energy diagram of OH addition reaction to C_{20}. The values are calculated at the B3LYP/6-311G(d,p) level. The B3LYP/6-31G(d) values are given in parenthesis.

spin density of OH radical is vanished in the addition to C_{20}, namely, almost all unpaired electron is transferred from OH to C_{20} by the addition.

3.3. Interaction of C_{20}(OH) with the OH radical

To elucidate affinity of OH radical in C_{20}, the first and second radical additions to C_{20} were calculated at the B3LYP/6-311G(d,p) and 6-31G(d) levels. Six addition sites (2-7) were examined as the second addition to C_{20}. The first OH radical is connected to C_1 atom, and the second OH radical binds to C_2-C_7 atoms. These sites are expressed by (1-2), (1-3), (1-4), and (1-7). The relative energies of the bind sites are given in Table 2. The second OH radical prefers the neighbor carbon atom (C_2) and the opposite carbon atom (C_7).

Table 2. Total energies (in Hartree) ite dependence of relative energies (ΔE in kcal/mol). The calculations were carried out at the B3LYP/6-31G(d) level.

Site	ΔE
1–2	0.00
1–3	6.45
1–4	8.46
1–5	4.13
1–6	31.67
1–7	3.71

Table 3. Spin densities on carbon atoms of C_{20}(OH).

atom	B3LYP/6–311G(d,p)
C1	−0.01
C2	0.46
C3	−0.09
C4	0.02
C5	0.06
C6	−0.12
C7	0.42

Spin densities on the carbon atoms of C_{20}(OH) are given in Table 3. It was found that the carbon atoms, C_2 and C_7, have high spin densities. Therefore, the second OH radical binds preferentially to C_2 and C_7 atoms of C_{20}(OH) because the radical-radical recombination is energetically favored.

The energy diagram of the OH radical addition to C_{20} is illustrated in . The binding energies of the first and second OH additions were calculated to be 85.2 kcal/mol and 91.5 kcal/mol, respectively. The second addition is more favored than the first addition.

4. Conclusion

In the present study, the DFT method has been applied to the interaction system between OH radical and smallest fullerene C_{20}. The DFT calculation showed that the OH radical binds directly to the carbon atom of C_{20} and a strong C-O bond is formed. The binding energies of the first addition of OH radical were calculated to be 85.2 kcal/mol at the B3LYP/6-311G(d,p) level of theory. In the second radical addition, the binding energy of OH to C_{20}(OH) was 91.5 kcal/mol. The unpaired electron was distributed widely over the C_{20} surface in the C_{20}(OH) complex.

Acknowledgment

This work is partially supported by the SUHARA memorial foundation. One of the authors (H.T) also acknowledges a partial support from a Grant-in-Aid for Scientific Research (C) from the Japan Society for the Promotion of Science (JSPS) (Project No. 21550002).

References

[1] Jensen, A. W., Wilson, S. R., & Schuster, D. I. (1996). *Bioorg. Med. Chem. 4*, 767.
[2] Chiang, L. Y., Lu, F. J., & Lin, J. T. (1995). *J. Chem. Soc., Chem. Commun.*, 1283.
[3] Zhu, Y. S., Sun, D. Y., Liu, G. Z., Liu, Z. Y., & Zhan, R. Y., & Liu, S. Y. (1996). *Chem. J. Chin. Univ. 17* 1127 (in Chinese).
[4] Lu, C. Y., Yao, S. D., Lin, W. Z., Wanga, W. F., Lin, N. Y., Tong, Y. P., & Rong, T. W. (1998). *Radiat. Phys. Chem.*, *53*, 137.
[5] Zeynalov, E. B., Allen, N. S., & Salmanova, N. I. (2009). *Poly. Degradat. Stabil.*, *94*, 1183.
[6] Parasuk, V. & Almlof, J. (1991). *Chem. Phys. Lett. 184*, 187–190.
[7] Frisch, M. J., et.al. (2003). Ab-initio MO calculation program: Gaussian 03, Revision B.04, Gaussian, Inc.: Pittsburgh PA.
[8] Tachikawa, H. & H. Kawabata, H. (2009). *J. Phys. Chem. C*, *113*, 7603.

[9] Tachikawa, H. (2008). *J. Phys. Chem. C.*, *112*, 10193.
[10] Tachikawa, H. (2007). *J. Phys. Chem. C.*, *111*, 13087.
[11] Tachikawa, H. & Shimizu, A. (2006). *J. Phys. Chem. B*, *110*, 20445.
[12] Iyama, T., Kawabata, H., & Tachikawa, H. (2007). *Mol. Cryst. Liqud Cryst.*, *472*, 697.
[13] Tachikawa, H., & Iyama, T., Abe, S. (2011). *Phys. Proc.*, *14*, 139.
[14] Tachikawa, H. (2011). *Phys. Chem. Chem. Phys.*, *13*, 11206.
[15] Tachikawa, H. (2011). *Phys. Chem. Chem. Phys.*, *13*, 5881.
[16] Tachikawa, H., Iyama, T., & Azumi, K. (2011). *Jpn. J. Appl. Phys.*, *50*, 01BJ03.
[17] Tachikawa, H. (2011). *Chem. Phys. Lett.*, *513*, 94.